Chemistry of Phosphido-Bridged Palladium(I) Dimers. η² Pd–H–P Interactions: A New Bonding Mode for Secondary Phosphines

Piero Leoni*

Scuola Normale Superiore, Piazza dei Cavalieri 7, I-56100 Pisa, Italy

Marco Pasquali* and Milena Sommovigo

*Department of Industrial Chemistry, University of Pisa,
Via Risorgimento 35, I-56126 Pisa, Italy*

Franco Laschi and Piero Zanello

Department of Chemistry, University of Siena, Piano dei Mantellini 44, I-53100 Siena, Italy

Alberto Albinati* and Francesca Lianza

Chemical Pharmacy, University of Milan, I-20131 Milan, Italy

Paul S. Pregosin* and Heinz Rüegger

Inorganic Chemistry, ETH-Zentrum, CH-8092 Zürich, Switzerland

The preparation of two new and unusual cationic Pd(I) dimeric complexes, containing bridging PBu$^t_2$ and terminal PHBu$^t_2$ ligands, is described. One of these, [Pd$_2$(μ-PBu$^t_2$)(μ-PHBu$^t_2$)-(PHBu$^t_2$)$_2$]$^+$, [2]$^+$, contains a Pd–H–P bridging unit, the first example of this type of bonding. A second, [Pd$_2$(μ-PBu$^t_2$)(CO)$_2$(PHBu$^t_2$)$_2$]$^+$, [3]$^+$, represents a rare example of a Pd(I) complex with terminal CO ligands. Electrochemical, ESR, one- and two-dimensional multinuclear NMR, and X-ray crystallographic studies have been carried out on both [2]$^+$ and [3]$^+$. Relevant crystallographic parameters for the two triflate complexes: compound [2a]$^+$ triclinic space group P$\bar{1}$, a = 10.245(1) Å, b = 10.739(1) Å, c = 22.624(3) Å, α = 79.816(9)°, β = 87.876(10)°, γ = 68.266(8)°, V = 2274.7(5) Å^3, Z = 2; compound [3a]$^+$ orthorhombic, space group Pbca, a = 21.910(7) Å, b = 21.120(3) Å, c = 16.625(8) Å, V = 7707(4) Å^3, Z = 8.

Introduction

Although the preparation and reaction chemistry of dimeric and monomeric compounds of Pd(I) is not widespread, there is increasing interest in this chemistry.[1–7] These dinuclear complexes often have bridging ligands, e.g. CO,[4] olefins,[5] and acetylenes,[6] as an important structural feature. Further, there is now a rare example of an ipso aryl carbon as a pseudobridging ligand[3] and, recently, the first example of a phosphido-bridged Pd(I) dimer has appeared.[2]

Normally, homogeneous catalysts based on palladium[8,9] are associated with the 0 and +2 oxidation states; however, preparative methods to afford new neutral and cationic monomeric as well as dinuclear palladium(I) materials should be welcome in that they may provide access to

otherwise inaccessible starting materials. To this end, we have reported[10] a high-yield synthesis of the dimeric secondary phosphine phosphido-bridged complex [Pd$_2$-(μ-PBu^t)$_2$(PHBu^t)$_2$], 1, and determined its molecular structure. In view of the good donor properties of the ligands in 1, this compound is expected to be a useful material for reactions with electrophiles. Indeed, as we began our studies, we considered that protonation of 1 would prove to be a simple way into relatively unexplored palladium hydride chemistry.[11,12] Generally speaking, there is a rich chemistry of dinuclear phosphido-bridged dimers.[13]

(1) Balch, A. L. *Comments Inorg. Chem.* 1984, 3, 51.

(2) Arif, A. M.; Heaton, D. E.; Jones, R. A.; Nunn, C. M. *Inorg. Chem.* 1987, 26, 4228.

(3) Budzelaar, P. H. M.; van Leeuwen, P. W. N. M.; Roobeck, C. F. *Organometallics* 1992, 11, 23.

(4) Portnoy, M.; Frolow, F.; Milstein, D. *Organometallics* 1991, 10, 3960.

(5) Wilson, W. L.; Nelson, J. H.; Alcock, N. W. *Organometallics* 1990, 9, 1699.

(6) Connelly, N. G.; Geiger, W. E.; Orpen, A. G.; Orsini, J. J.; Richardson, K. E. *J. Chem. Soc., Dalton Trans.* 1991, 2967.

(7) Miedaner, A.; Haltiwanger, R. C.; DuBois, D. L. *Inorg. Chem.* 1991, 30, 417.

(8) (a) Yoshida, T.; Matsuda, T.; Okano, T.; Kitami, T.; Otsuka, S. *J. Am. Chem. Soc.* 1979, 101, 2027. (b) Jensen, C. M.; Trogler, W. C. *J. Am. Chem. Soc.* 1986, 108, 723. (c) Trogler, W. C. *Science (Washington, D.C.* 1986, 233, 1538. (d) Benn, R.; Jolly, P. W.; Mynott, R.; Schenker, G. *Organometallics* 1985, 4, 1136. (e) Neilan, J. P.; Laine, R. M.; Cortese, N.; Heck, R. F. *J. Org. Chem.* 1976, 41, 3455. (f) Knifton, J. F. *J. Org. Chem.* 1976, 41, 2885. (g) Guibe, F. *J. Org. Chem.* 1981, 46, 4439. (h) Baillargeon, V. P.; Stille, J. K. *J. Am. Chem. Soc.* 1983, 105, 7175.

(9) (a) Yamamoto, T.; Yamamoto, A. *Tetrahedron Lett.* 1982, 23, 3383. (b) Alper, H.; Woell, J. B.; Despeyroux, B.; Smith, D. J. H. *J. Chem. Soc., Chem. Commun.* 1983, 1270. (c) Alper, H.; Leonard, D. *J. Chem. Soc., Chem. Commun.* 1985, 511. (d) Fenton, D. M. *J. Org. Chem.* 1974, 39, 701. (e) Rivetti, F.; Romano, U. *Chem. Ind.* 1980, 62, 7. (f) Rivetti, F.; Romano, U. *J. Organomet. Chem.* 1978, 154, 323.

(10) Pasquali, M.; Sommovigo, M.; Leoni, P.; Sabatino, P.; Braga, D. *J. Organomet. Chem.* 1992, 423, 263.

(11) Di Bugno, C.; Pasquali, M.; Leoni, P.; Sabatino, P.; Braga, D. *Inorg. Chem.* 1989, 28, 1390.

1, R = Bu^t
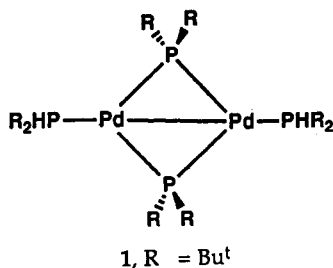
We report here (a) the preparation of two unusual hydrido and carbonyl derivatives of 1 as well as (b) their characterization via X-ray diffraction and 1- and 2-D NMR measurements plus (c) aspects of the electrochemistry of these new complexes. Part of this work has been previously communicated.[14]

Results and Discussion

Synthesis and Characteristics of the η^2 Cationic Complex [2]+. Reaction of 1 with CF_3SO_3H or HBF_4–Et_2O in dimethoxyethane for 2 h followed by addition of ether gave [2]+ in good yield, as shown in eq 1. The solution

X = CF$_3$SO$_3$, [2a]$^+$

X = BF$_4$, [2b]$^+$
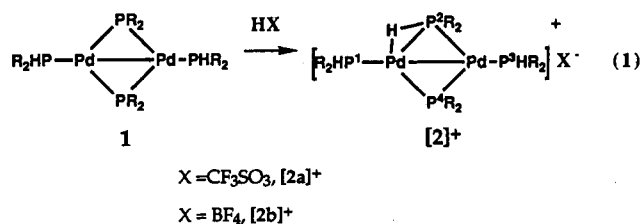
structure proof for [2a]+ has been presented earlier[14] so that only a brief summary will be repeated here: (1) The ^{31}P spectrum shows *four* groups of signals due to the different types of phosphorus environment which arise when the complex symmetry is lowered, with two coordinated secondary phosphines at relatively high field, 47.7 and 52.0 ppm, and two bridging phosphides appearing at relatively low field, 217.2 and 455.3 ppm. Such low-field positions for bridging phosphides are known.[2,13,15] (2) The two secondary phosphine protons appear at 4.92 and 5.16 ppm, with their usual[16] large one-bond interactions, 322 and 324 Hz, respectively. (3) In the proton spectrum, the "hydridic" type proton is found at $\delta = -0.16$ ppm as a doublet of doublets, due to a relatively large (but reduced) 151-Hz one-bond coupling to P2, the bridging phosphorus at 217.2 ppm, and a smaller coupling to P4, the other bridging phosphorus at 455.3 ppm. (4) Heteronuclear Overhauser experiments (1- and 2-D) reveal a strong interaction between P2, the phosphorus with the large one-bond interaction, and the "hydride".

Figure 1. Sections of the phase-sensitive 5.9-T $^{31}P-^{1}H$ correlation spectrum for [2]+. Negative signals are drawn with a single contour, whereas positive signals are shown with multiple levels. (A) Region of the terminal secondary phosphines. (B) and (C) Regions of the bridging phosphine, P2, and the phosphide, P4, respectively.

The keys to the structure proof stem from points 3 and 4. One must know which ^{31}P spin shows the large coupling to the hydride, and this assignment follows from a phase-sensitive 2-D $^{31}P,^{1}H$ correlation (see Figure 1); one must also know whether this phosphorus spin is close in space to the hydride, and this information comes from heteronuclear Overhauser spectroscopy.[17] Given these data, one can rule out a terminal hydride such as
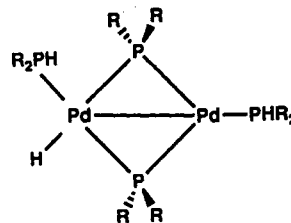
In view of some ambiguities connected with the X-ray diffraction study on [2a]+, we have measured the solid-state ^{31}P CP/MAS NMR spectrum for this material. There are four different environments in agreement with the solution data, so that we feel confident that the structure is the same in both states. This solid-state spectrum is not trivial since (a) there are two nonequivalent molecules in the unit cell and (b) the two phosphido resonances are very anisotropic so that our spinning rate of 15 kHz was insufficient to remove all of the spinning side bands; see Figure 2. The same figure shows the result of changing the contact time, i.e., allowing the proton only a limited

(12) (a) Leoni, P.; Sommovigo, M.; Pasquali, M.; Midollini, S.; Braga, D.; Sabatino, P. *Organometallics* 1991, *10*, 1038. (b) Sommovigo, M.; Pasquali, M.; Leoni, P.; Sabatino, P.; Braga, D. *J. Organomet. Chem.* 1991, *418*, 119.

(13) (a) Powell, J.; Sawyer, J. F.; Stainer, M. V. R. *Inorg. Chem.* 1989, *28*, 4461. (b) Powell, J.; Sawyer, J. F.; Smith, S. J. *J. Chem. Soc., Chem. Commun.* 1985, 1312. (c) Powell, J.; Gregg, M. R.; Sawyer, J. F.; *Chem. Soc., Chem. Commun.* 1987, 1029. (d) Blum, T.; Braunstein, P. *Organometallics* 1989, *8*, 2497. (e) Colbran, S. B.; Johnson, B. F. G.; Lewis, J.; Sorrel, R. M. *J. Organomet. Chem.* 1985, *296*, C1.

(14) Albinati, A.; Lianza, F.; Pasquali, M.; Sommovigo, M.; Leoni, P.; Pregosin, P. S.; Ruegger, H. *Inorg. Chem.* 1991, *30*, 4690.

(15) Adams, M. R.; Gallucci, J.; Wojcicki, A.; Long, G. L. *Inorg. Chem.* 1992, *31*, 2. Powell, J.; Fuchs, E.; Gregg, M. R.; Phillips, J.; Stainer, M. V. R. *Organometallics* 1990, *9*, 387.

(16) Bentrude, W. G.; Setzer, W. N. In *Methods in Stereochemical Analysis*; Verkade, J. G., Quin, L. D., Eds.; VCH: New York, 1987; Vol. 8, p 35.
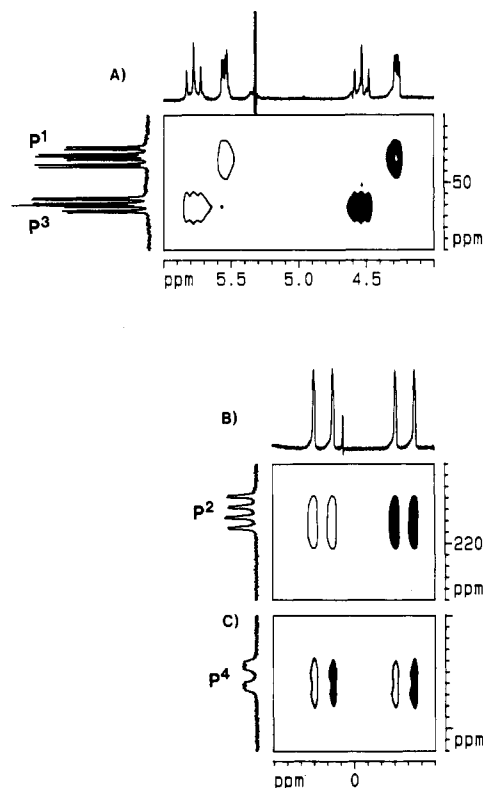
(17) Pregosin, P. S. In *Methods in Stereochemical Analysis*; Verkade, J. G., Quin, L. D., Eds.; VCH: New York, 1987; Vol. 8, p 465.
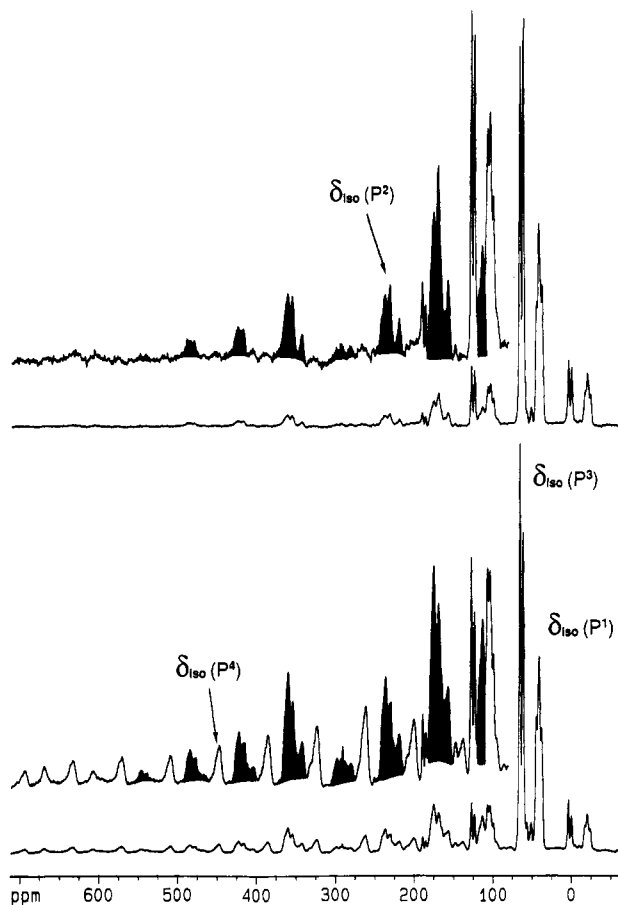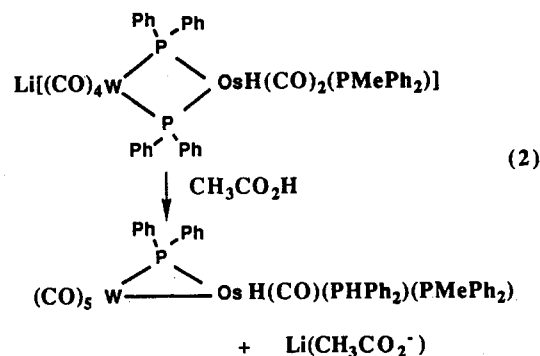
Figure 2. ^{31}P CP/MAS spectra for [2]$^+$ recorded at 162.0 MHz with ν_{rot} = 10 kHz. The resonances of the bridging phosphine, P2, are marked in black. Lower traces: CP time = 8 ms. All phosphorus resonances are visible. Upper traces: CP time = 80 μs. Only the protonated phosphorus atoms show up.

amount of time to transfer magnetization. The ^{31}P signal not having a proton close by, i.e. the bridging phosphide, P4, loses intensity, and this further confirms that P2 is a bridging phosphide in close contact with a proton. We note that there is a growing literature[18] on solid-state ^{31}P results in metal complexes but few on bridging phosphides.[19]

The novelty of complex [2]$^+$ is *both* structural and chemical, chemical in that protonation of bridging phosphides usually gives hydride complexes.[13,20] And this is especially true for heteronuclear monophosphido-bridged molecules. For diphosphido compounds there is at least one case (see eq 2), in which the bridge phosphorus is protonated.[20,21] Compound [2]$^+$ is structurally novel, in that this is the first example of an "agostic" interaction[22]

involving an M---H-P fragment. Bridging hydrides[23] and borohydrides[24] are now well-known, as are interactions of C-H bonds;[22] even a few M---H-N interactions have been found[25] (the identification of which now rests, in part, on $^1J(N,H)$ values[26]). However, this represents the first such bond in which a phosphorus atom is involved. In connection with our structure we note the recent report by Braunstein and co-workers[27] on the reaction of [Pt$_2$(μ-PPh$_2$)$_2$(PPh$_3$)$_2$] with the gold cation AuPPh$_3^+$. The resulting tetrameric product was shown to possess a Pt-Au-P(phosphido) unit, rather than a Pt-Au-Pt arrangement. Fragment molecular orbital analysis showed[27] that the shape of the HOMO orbitals of the Pt dimers favors attack of the incoming AuPPh$_3^+$ on the phosphido Pt-P bond rather than the Pt-Pt bond, and this is interesting for us given the isolobal relationship between H$^+$ and AuPPh$_3^+$.

In the course of our structural characterization, we noticed an interesting and selective dynamic property of [2]$^+$. Both ^{31}P and ^1H-2D EXSY measurements[28,29] (see Figure 3 for one example) show that the two nonequivalent terminal secondary phosphine ^{31}P (and ^1H) signals are involved in a slow exchange process with one another at ambient temperature. There is neither ^1H hydride proton–secondary phosphine proton nor ^{31}P phosphide–phosphide exchange. These results can be explained as shown in Scheme I.

The top route (dotted arrows) accounts for the EXSY results in that the proton does not dissociate but rather moves across one side of the Pd-Pd bond, perhaps via a complex containing a bridging secondary phosphine. A mechanism in which we move the protonated bridging phosphide into a terminal position (bottom route, solid arrows), thus creating two terminal secondary phosphines on one palladium, is also possible but only if the newly

(18) Fyfe, C. A. *Solid-State NMR for Chemists*; CFC Press: Guelph, Ontario, Canada, 1983.

(19) Carty, A. J.; Fyfe, C. A.; Lettinga, M.; Johnson, S.; Randall, L. H. *Inorg. Chem.* **1989**, *28*, 4120.

(20) Rosenberg, S.; Geoffroy, G. L.; Rheingold, A. L. *Organometallics* **1985**, *4*, 1184. Werner, H.; Hofman, W.; Zolk, R.; Dahl, L. F.; Kocal, J.; Kuhn, A. *J. Organomet. Chem.* **1985**, *289*, 173. (b) Adatia, T.; McPartlin, M.; Mays, M. J.; Morris, M. J.; Raithby, P. R. *J. Chem. Soc., Dalton Trans.* **1989**, 1555.

(21) Shyu, S.; Wojcicki, A. *Organometallics* **1984**, *3*, 809.

(22) (a) Brookhart, M.; Green, M. L. H. In *Progress in Inorganic Chemistry*; Lippard, S. J., Ed.; Wiley Interscience: New York, 1988; Vol. 36, p 1. (b) Albinati, A.; Pregosin, P. S.; Wombacher, F. *Inorg. Chem.* **1990**, *29*, 1812.

(23) (a) Venanzi, L. M. *Coord. Chem.* **1981**, *21*, 151. (b) Albinati, A.; Lehner, H.; Venanzi, L. M.; Wolfer, M. *Inorg. Chem.* **1987**, *26*, 3933. (c) Pregosin, P. S.; Togni, A.; Venanzi, L. M. *Angew. Chem.* **1981**, *93*, 684. (d) Leoni, P.; Grilli, E.; Pasquali, M.; Tomassini, M. *J. Chem. Soc., Dalton Trans.* **1986**, 1041.

(24) (a) Marks, T. J.; Kolb, J. R. *Chem. Rev.* **1977**, *77*, 26. (b) Bau, R.; Yuan, H. S. H.; Baker, M. V.; Field, L. D. *Inorg. Chim. Acta* **1986**, *114*, L27.

(25) (a) Heddon, D.; Roundhill, D. M.; Fultz, W. C.; Rheingold, A. L. *Organometallics* **1986**, *5*, 336. (b) Wehman, I. C. M.; Grove, D. M.; Van der Sluis, P.; Speck, A. L.; Van Koten, G. *J. Chem. Soc., Chem. Commun.* **1990**, 1367. (c) Brammer, L.; Charnock, J. M.; Goggin, P. L.; Goodfellow, R. J.; Orpen, A. G.; Koetzle, T. F. *J. Chem. Soc., Dalton Trans.* **1991**, 1789.

(26) Pregosin, P. S.; Ruegger, H.; Wombacher, F.; van Koten, G.; Grove, D. M.; Wehman-Ooyevaar, *Magn. Reson. Chem.* **1992**, *30*, 548.

(27) Bender, R.; Braunstein, P.; Dedieu, A.; Dusausay, Y. *Angew. Chem., Int. Ed. Engl.* **1989**, *28*, 923.

(28) Ammann, C. J.; Pregosin, P. S.; Ruegger, H.; Grassi, M.; Musco, A. *Magn. Reson. Chem.* **1989**, *27*, 355.

(29) Albinati, A.; Kunz, R. W.; Ammann, C. J.; Pregosin, P. S. *Organometallics* **1991**, *10*, 1800.
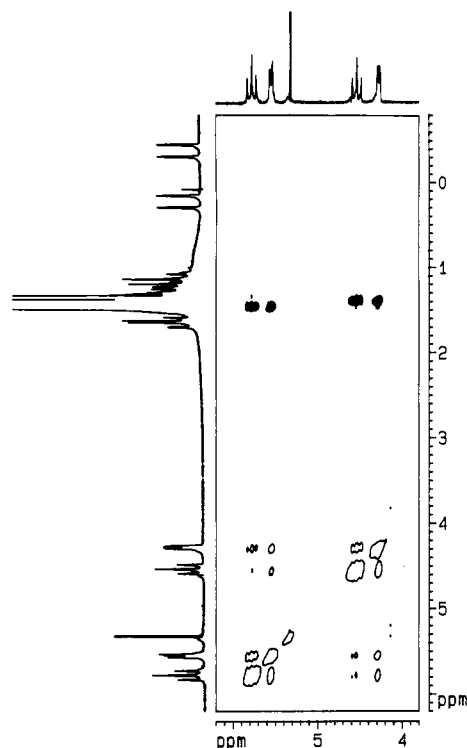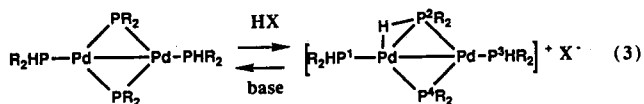
Figure 4. ORTEP view of the molecular structure of [2]+.

Figure 3. ¹H NOESY spectrum for [2]+ recorded at 250 MHz. NOE cross peaks (opposite in phase relative to the diagonal) are visible between the hydrogens at the terminal secondary phosphines and the respective *tert*-butyl groups, whereas chemical exchange occurs only among the terminal PH protons and does not involve the bridging phosphine at $\delta = -0.16$ ppm.

Scheme I
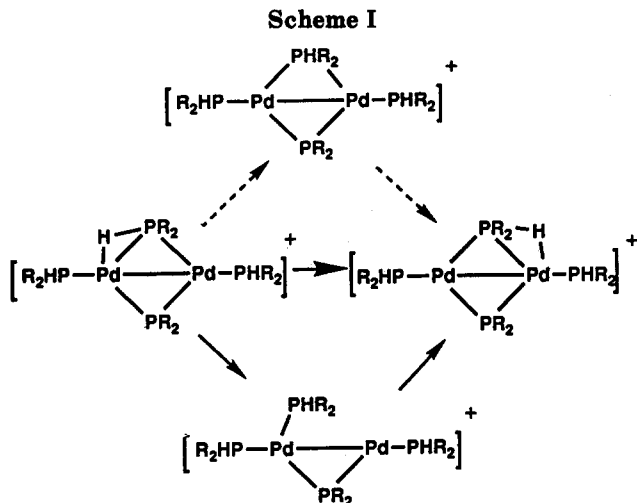
protonated ligand is the one which returns to the bridging position. Both of these processes exchange the two secondary phosphine ³¹P signals, but not the phosphide resonances. In a similar vein, one exchanges the two secondary phosphine protons, but not the "hydride" with the phosphine P–H. The reaction of 2 with bases of differing strength, e.g. Ph₃C⁻, H⁻, and imidazole

affords quantitative formation of 1, in all cases, with no trace of products arising from substitution of either

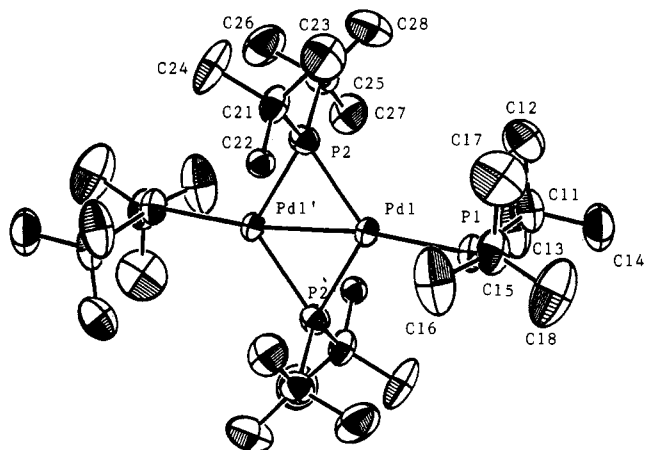coordinated phosphide or phosphine. This chemistry is interesting and parallels our observations[11b] on the reversible deprotonation of the cationic hydride complex *trans*-PdH(H₂O)(PCy₃)₂+.

Comments on the Solid-State Structure of [2a]+. The structure of [2a]+, as imposed by the crystallographic symmetry, does not correspond to the molecular symmetry. There are effectively two half-independent molecules in the unit cell; i.e., each dimer lies across a center of symmetry. Since it was not possible to locate the hydride, we restrict our comments to the bond distances and bond angles associated with the heavy atoms and show an appropriate ORTEP plot in Figure 4. The most important (averaged) structural features concern the Pd–Pd separation, 2.611(1) Å, the nonequivalent Pd–P(bridge) distances, Pd–P2, 2.393(2) Å, and Pd–P2′, 2.313(2) Å, as well as the angles P1–Pd–P2, 134.4(7)°, P1–Pd–P2′, 113.0(8)°, and Pd–P2–Pd, 67.4°, thereby defining the coordination sphere. We note the recent[2] structure for the symmetrical dimer [Pd₂(μ-PBuᵗ₂)₂(PMe₃)₂] in which one finds a metal–metal separation of 2.571(2) Å as well as a Pd–PBuᵗ distance of 2.329(3) Å. Further, preliminary[12b] X-ray data for the secondary phosphine complex 1 show a Pd–Pd distance of 2.594(1) Å as well as a Pd–PBuᵗ separation of 2.336(2) Å. The angles P(terminal)–Pd–P(bridging) for these two model complexes are 123.5(6) and 116(1)°, respectively. Our P1–Pd–P2 angle of ca. 134° and the longer Pd–P2 distance are consistent with an opening due to the presence of a bridging Pd–H–P unit (whose structure we have proven via NMR).

Preparation and Characteristics of the Cationic Carbonyl Compounds [3]+. Reaction of a dimethoxyethane solution of either [2a]+ or [2b]+ with 1 atm of CO at room temperature leads to the complex [Pd₂(μ-PBuᵗ₂)-(CO)₂(PHBuᵗ₂)₂]X, 3, X = CF₃SO₃⁻, a, or BF₄⁻, b. The reaction to form [3a]+ is also an equilibrium and lies ca. 90% to the right under the reaction conditions, as demonstrated by UV–vis spectroscopy. The complex can be isolated in an analytically pure form as a yellow crystalline material, although in poor yield due to the tendency of [2a]+ to cocrystallize. Better yields are obtained if the reaction is carried out in the presence of excess CF₃SO₃H, which protonates the PHBuᵗ₂ set free, thereby shifting the equilibrium to the right; however, the resulting phosphonium salt often contaminates [3a]+. The same chemistry with the fluoroborate analog, [2b]+, as starting material was more rewarding in terms of yield of pure [3b]+ due to the differing solubilities of the product
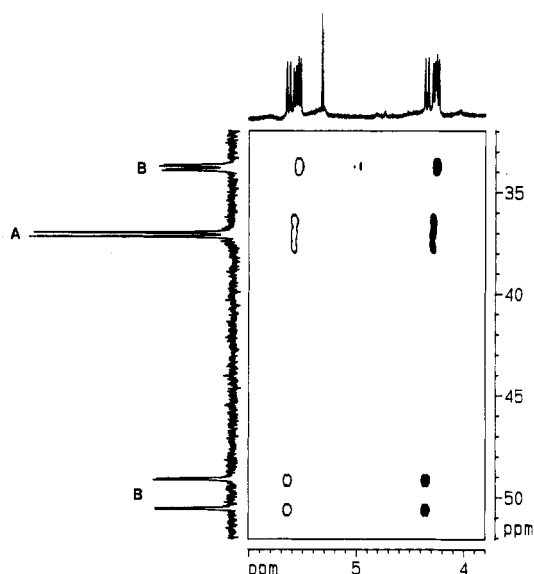
Figure 5. Section of the phase-sensitive $^{31}P,^1H$ correlation spectrum for [3]$^+$, showing the secondary phosphines in the trans isomer (A) and cis isomer (B).
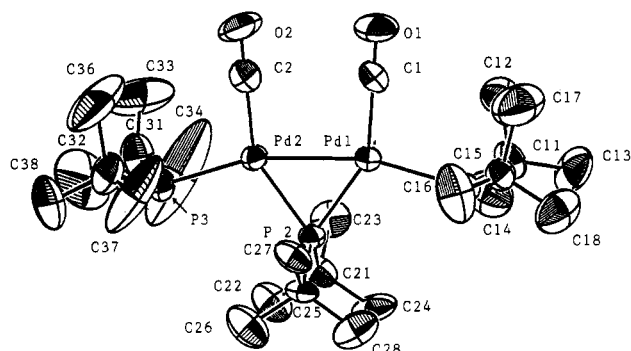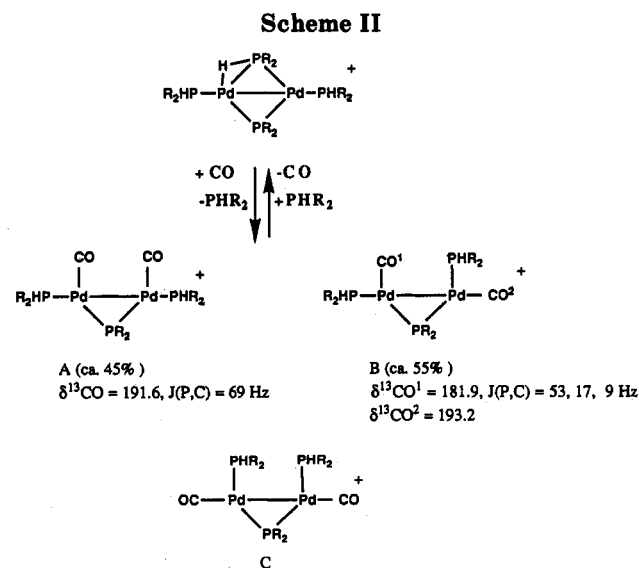

Figure 6. ORTEP view of the trans isomer of [3]$^+$.

Scheme II

A (ca. 45%)
$\delta^{13}CO = 191.6$, J(P,C) = 69 Hz

B (ca. 55%)
$\delta^{13}CO^1 = 181.9$, J(P,C) = 53, 17, 9 Hz
$\delta^{13}CO^2 = 193.2$

C

and phosphonium salt. Complex [3a]$^+$ represents the first palladium(I) dimer with terminal CO ligands to be characterized crystallographically (see below) and shows CO IR stretches at 2080, 2055, and 2045 cm^{-1}.

In solution the carbonyl dimer, [3a]$^+$, shows five ^{31}P types, suggestive of a mixture of isomers, as shown in Scheme II. The trans isomer, A (with respect to the secondary phosphines), should reveal two ^{31}P signals in

Table I. Selected Bond Distances (Å) and Angles (deg) in [2a]$^+$ and [3a]$^+$

Compound [2a]$^+$

	molecule 1	molecule 2
Pd–Pd'	2.611(1)	2.611(1)
Pd–P1	2.330(2)	2.324(2)
Pd–P2	2.393(2)	2.391(2)
Pd–P2	2.311(2)	2.315(2)
P–C (average)	1.880(9)	1.882(10)
P1–Pd–P2	133.9(1)	134.9(1)
P1–Pd–P2''	113.5(1)	112.4(1)
P2–Pd–P2'	112.6(1)	112.6(1)
Pd–P2–Pd'	67.4(1)	67.4(1)

Compound [3a]$^+$

Pd1–Pd2	2.682(1)	Pd1–C1	1.93(2)
Pd1–P1	2.355(4)	Pd2–C2	1.93(2)
Pd2–P3	2.348(3)	C1–O1	1.14(2)
Pd1–P2	2.274(4)	C2–O2	1.15(2)
Pd2–P2	2.271(4)	P–C (average)	1.88(3)
P1–Pd1–P2	110.1(1)	P2–Pd1–C1	148.6(5)
P2–Pd2–P3	109.7(1)	P2–Pd2–C2	149.3(5)
Pd1–P2–Pd2	72.3(1)	P3–Pd2–C2	100.9(5)
P1–Pd1–C1	101.1(5)		

the form of an AX_2 spin system (assuming proton decoupling), and this is observed (363.0 and 38.1 ppm, $^2J(P,P) = 20$ Hz), whereas the cis isomer, B, should show three ^{31}P environments and afford a typical first-order AMX spin system, and this is found as well (380.4 ppm, $^2J(P,P) = 147$ and 22 Hz, 50.4 ppm, $^2J(P,P) = 147$ and 7 Hz, and 34.7 ppm, $^2J(P,P) = 22$ and 7 Hz). The cis isomer, provides a useful model for the $^{31}P,^{31}P$ couplings in these molecules. We find a large $^2J(P,P)$ coupling of 147 Hz and assign this to the coupling arising from a pseudo-trans orientation of the phosphide and one of the secondary phosphine ^{31}P spins. The smaller coupling of ca. 22 Hz is assigned to the pseudo-cis interaction. These background data allow us to assign the more symmetrical structure to the isomer with trans phosphines (structure A), as shown, since the compound with trans CO ligands (structure C) must show the large $^2J(P,P)$ coupling and this is not observed, in agreement with the structural result. ^{13}CO NMR data for the mixture are also shown in the scheme.

The proton spectrum of [3]$^+$ shows the PH protons between 4.0 and 5.8 ppm, centered at ca. 5.0 ppm. These can be unequivocally assigned via the $^{31}P,^1H$ 2-D correlation shown in Figure 5. The large spread of the phosphorus cross peaks for the ^{31}P resonance at ca. 37 ppm, arising from isomer A, is indicative of a second-order spin system. As expected, there are no signals in the hydride region.

All attempts to obtain a complex containing a bridged CO failed (see Experimental Section). As the reaction in Scheme II is reversible, we conclude that a bridging phosphine in [2]$^+$ and the carbonyl ligands in [3]$^+$ are relatively labile and that both compounds should allow ready access to the coordinatively unsaturated dinuclear cation [4]$^+$. We believe that both [2]$^+$ and [3]$^+$ are
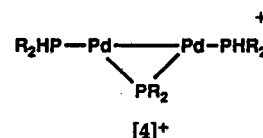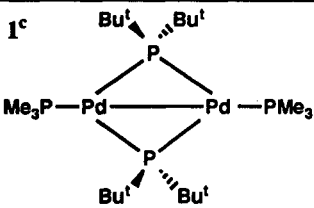

[4]$^+$
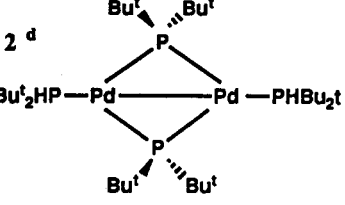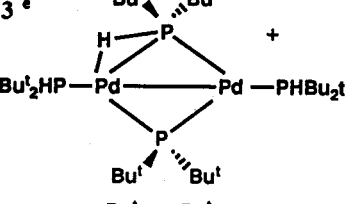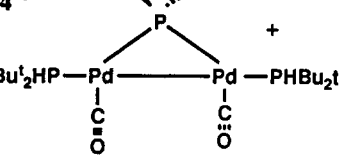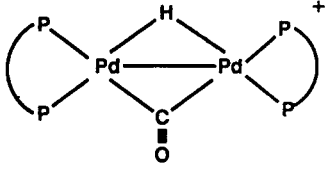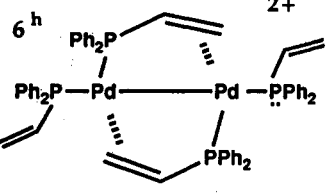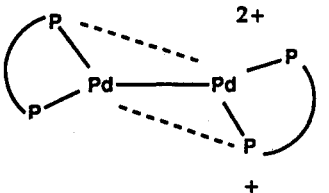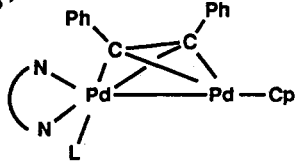
Table II. Selected X-ray Data for Model Complexes[a,b]

	Pd–Pd	Pd–P	P(T)–Pd–P(B)	Pd–P(B)–Pd
1[c]	2.571(2)	2.250(5) T 2.329(3) B	123.5(1)	67.0(1)
2[d]	2.594(1)	2.287(2) T	116.9(1)	
3[e]	2.611(1)	2.327(2) T 2.392(2) B 2.313(2) B	112.9(7) 134.3(8)	67.4(3)
4[f]	2.682(1)	2.350(2) T 2.275(3) B	109.8(3)	72.3(1)
5[g]	2.767(4)	2.369(4) 2.328(4)	(trans to CO) (trans to H)	
6[h]	2.748(2)	2.328(6) T 2.255(2) B		
7[i]	2.701(3)	2.329(4) T 2.235(4) B 2.690(4) B		
8[j] L = nothing L = CH₃CN L = P(POPh)₃	2.541(3) 2.571(3) 2.622(3)			

^{a} T = terminal, B = bridging; distances in angstroms, angles in degrees. ^{b} Chelate in entry 5 = 1,3-bis(diisopropylphosphino)propane. Chelate in entry 7 = 1,3-bis(diphenylphosphino)propane. ^{c} Data from ref 2. ^{d} Data from ref 12. ^{e} This work. ^{f} This work. ^{g} Data from ref 4. ^{h} Data from ref 5. ^{i} Data from ref 3. ^{j} Data from ref 6.

promising starting materials for reactions with unsaturated organic ligands and should prove interesting substrates for potential oxidative addition reactions. Naturally, one must keep in mind that basic substrates will deprotonate [2]⁺ affording 1.

X-ray Structure for [3a]⁺. The solid-state structure for [3a]⁺, as determined by X-ray diffraction, is shown as an ORTEP plot in Figure 6. Table I contains a selected list of bond angles and bond distances for both [2a]⁺ and [3a]⁺, and Table II shows a collection of bond lengths for known model Pd(I) dimeric compounds. Interestingly, the solid-state structure represents that for the less abundant, but more symmetrical, isomer, suggesting that [3a]⁺ (A) may crystallize preferentially from the solvent chosen.

The most interesting bond length concerns the Pd–Pd separation. As can be seen from comparison with the model complexes, the Pd–Pd distances in [2a]⁺ and [3a]⁺, 2.611(1) and 2.682(1) Å, respectively, are found in the middle of the range and do not seem to correlate with the overall charge on the complex (compare entry 5 with 6 as well as 4 with 7). The observed Pd–P(terminal) separations in both of our compounds are comparable to those found in other complexes, but the Pd–P(bridging) length in [3a]⁺ is somewhat short. The Pd–C distance for the two Pd–CO bonds in [3a]⁺ is 1.93(2) Å and the average CO separation is 1.15(2) Å, in keeping with a triple bond. The average P(terminal)–Pd–C angle is ca. 101°, and we assume that this deviation from 90° is steric in origin.

Electrochemistry and ESR Studies. Given the novelty of [2]⁺ and [3]⁺, we have carried out a few electrochemical experiments with the aim of obtaining further insight into the reactivity of our materials. There have been a few recent studies on Pd(I) dimers with respect to their ability to afford higher and mixed oxidation states,[30] and it is known that for certain phosphido Pt(I) dimers electrochemical reduction proceeds by an irreversible pathway.[31]

Figure 7 compares the electrochemical fingerprint of [2a]⁺ (top) with that of 1 (bottom), in tetrahydrofuran solution.

As can be seen, the cathodic scan relevant to [2a]⁺ shows the presence of a reduction process at peak A and, in the reverse direction, one finds a directly associated response at peak B, the peak height of which is notably lower than that of the parent peak A (i_{pB}/i_{pA} = 0.3). There is a further oxidation step at peak C which is absent in the direct anodic scan, and which displays a directly associated response, peak D, in the reverse scan. It is evident that this C/D profile is fully coincident with the response exhibited by 1, under the same experimental conditions, suggesting that the electrochemical reduction at peak A ultimately affords 1.

Controlled potential coulometric tests performed on a tetrahydrofuran solution of [2a]⁺ (E_w = -1.5 V) show the consumption of 1 electron/molecule. Concomitantly, the violet solution turns to brown and the precipitate which forms was identified as 1. Obviously, the chemically irreversible nature of the reduction process of [2a]⁺ does not involve rupture of the Pd–Pd bond and probably represents the release of the bridging hydride atom,
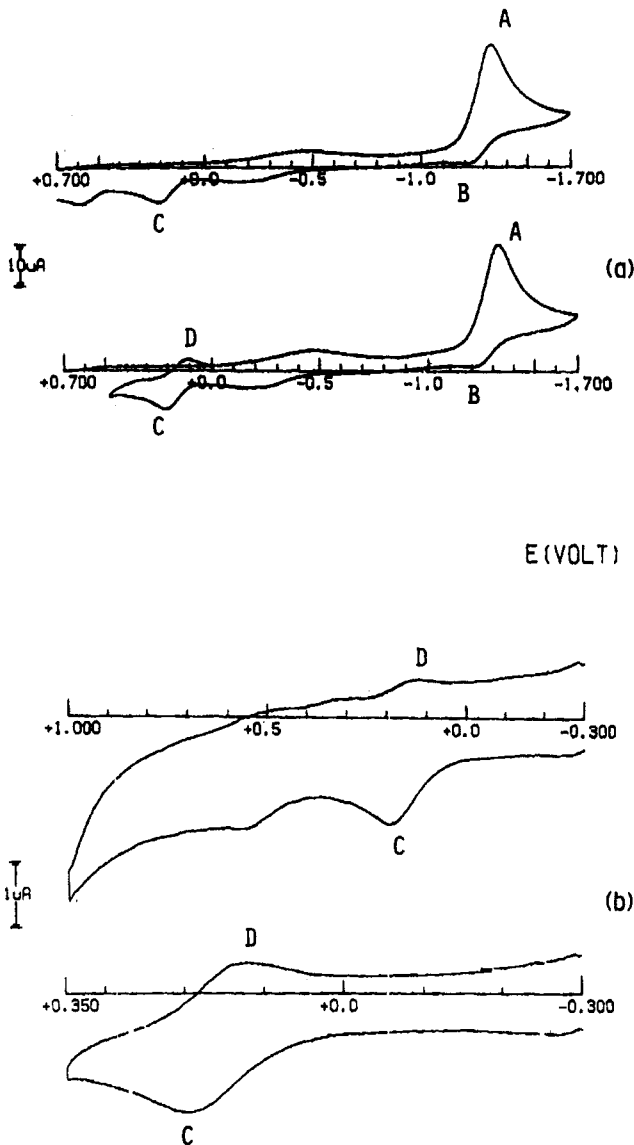
Figure 7. Cyclic voltammetric responses recorded at a platinum electrode on THF solutions containing [NBu₄]-[ClO₄] (0.2 mol dm⁻³) and [2a]⁺ (2.2 × 10⁻³ mol dm⁻³), top two traces, and 1 (saturated), bottom two traces. The scan rate was 0.2 V s⁻¹.

according the overall path

$$[2a]^+ \xrightarrow[E_p\ =\ -1.33\ V]{+e} 1 + \tfrac{1}{2}H_2 + CF_3SO_3^-$$
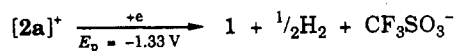
No attempt has been made to detect hydrogen gas although this is quite likely to be one of the products.

In Figure 8 one notes that the increase of the scan rate causes the i_{pB}/i_{pA} ratio to increase. At the highest explored scan rate (10.24 V s⁻¹) the peak current ratio reaches 0.7. This allows us to assign a lifetime ($t_{1/2}$) of about 0.1 s to the neutral transient species **2a**.[32] The peak-to-peak separation ($E_{pB} - E_{pA}$) gradually increases from 99 mV at 0.1 V s⁻¹ (at lower scan rates the return peak is absent) to 350 mV at 10.24 V s⁻¹. Under the same experimental conditions, the 1-electron oxidation of ferrocene ($E^{o\prime}$ = 0.54 V), which is known to cause minimal geometrical

(30) (a) Yao, C.-L.; He, L.-P.; Korp, J. D.; Bear, J. L. *Inorg. Chem.* **1988**, *27*, 4389. (b) Cotton, F. A.; Masutz, M.; Poli, R.; Feng, X. *J. Am. Chem. Soc.* **1988**, *110*, 1144. (c) Umakoshi, K.; Ichimura, A.; Kinoshita, I.; Ooi, S. *Inorg. Chem.* **1990**, *29*, 4005.
(31) Krevor, J. V. Z.; Yee, L. *Inorg. Chem.* **1990**, *29*, 4305.

(32) Brown, E. R.; Sandifer, J. R. In *Physical Methods of Chemistry. Electrochemical Methods*; Rossiter, B. W., Hamilton, J. F., Eds.; Wiley: New York, 1986; Vol. 2, Chapter 4.

E (VOLT)
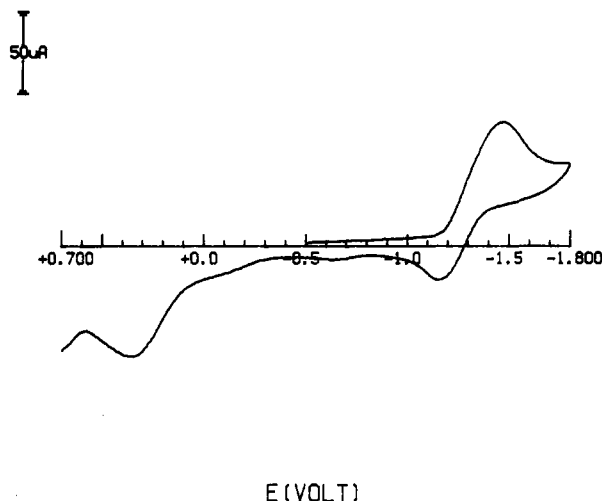
Figure 8. Cyclic voltammogram recorded under the same experimental conditions as for Figure 7 (upper trace), at a scan rate of 5.12 V s^{-1}.

rearrangements,[33-35] exhibits an increase in ΔE_p from 137 to 570 mV. This should suggest[36] that the conversion of [2a]$^+$ to the corresponding neutral species 2a does not involve major structural reorganization.

With respect to the structural rearrangement accompanying the 1-electron redox change 1/[1]$^+$, analysis of the cyclic voltammetric response relevant to the peak system C/D o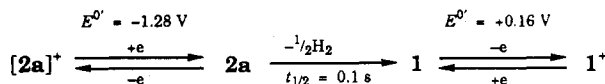f Figure 7 at scan rates ν varying from 0.02 to 1.00 V s^{-1} indicates that (a) the peak current ratio i_{pD}/i_{pC} is constantly equal to 1, (b) the peak-to-peak separation gradually increases from 66 to 103 mV (in the same scan rate range, the ΔE_p value for the oxidation of ferrocene increases from 78 to 343 mV), and (c) the current function $i_{pC}/\nu^{1/2}$ remains substantially constant. This oxidation, although slow, due to the poor solubility of 1, is chemically reversible (as shown by both CV and dc polarography on the same sample after 2 h), and we have seen no evidence of decomposition over several hours.

In summary, the redox paths exhibited by [2a]$^+$ and 1 leave the Pd/Pd frame intact and can be described as follows:

$$E^{0'} = -1.28 \text{ V} \qquad\qquad E^{0'} = +0.16 \text{ V}$$

$$[2a]^+ \underset{-e}{\overset{+e}{\rightleftarrows}} 2a \xrightarrow[t_{1/2} = 0.1 \text{ s}]{-^1/_2 H_2} 1 \underset{+e}{\overset{-e}{\rightleftarrows}} 1^+$$

Electrochemistry of [3]$^+$. The carbonyl, [3]$^+$, undergoes an irreversible 1-electron reduction process at E_p = -1.08 V and no oxidation step. Upon exhaustive 1-electron addition (E_w = -1.2 V), the starting yellow-brown solution turns to red-orange, but no clearly attributable redox fingerprint was detected by cyclic voltammetry. Perhaps substitution of the bridging P(Bu^t)$_2$ fragment by two terminal CO groups results in fragmentation to mononuclear species upon 1-electron addition.

X-Band EPR Analysis. In view of the nontransient nature of the paramagnetic cation [1]$^+$, we attempted its EPR characterization. Although we have no evidence for decomposition, to be on the safe side, [1]$^+$ was electro-
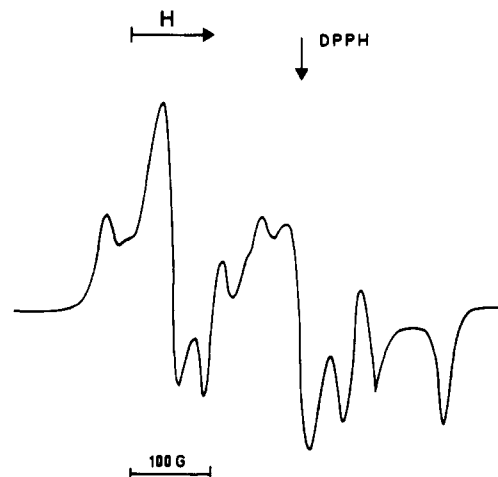
(33) Seiler, P.; Dunitz, J. D. *Acta Crystallogr.* 1979, *B35*, 1068.

(34) Churchill, M. R.; Landers, A. G.; Rheingold, A. L. *Inorg. Chem.* 1981, *20*, 849.

(35) Geib, S. J.; Rheingold, A. L.; Dong, T.-Y.; Hendrickson, D. N. *J. Organomet. Chem.* 1986, *312*, 241.

(36) Cinquantini, A.; Opromolla, G.; Zanello, P. *J. Chem. Soc., Dalton Trans.* 1991, 3161 and references therein.

Figure 9. X-Band EPR spectrum of the monocation [1]$^{2+}$ electrogenerated in THF solution. T = 100 K.

Table III. X-Band EPR Parameters of [1]$^+$ in THF Solution, at Liquid Nitrogen and Fluid Solution Temperature

g_l = 2.104 ± 0.005; g_m = 2.005 ± 0.005; g_h = 1.951 ± 0.005
$\langle g \rangle_{calc}$ = $^1/_3(g_l + g_m + g_h)$ = 2.020 ± 0.005
$a_l(^{31}P1)$ = 70 ± 5 G; $a_l(^{31}P2)$ = 48 ± 5 G
$a_m(^{31}P1)$ = 47 ± 5 G; $a_m(^{31}P2)$ = 32 ± 5 G
$a_h(^{31}P1)$ = 90 ± 5 G; $a_h(^{31}P2)$ = 40 ± 5 G
$\langle a \rangle_{calc}(^{31}P1)$ = $^1/_3(a_l + a_m + a_h)$ = 68 ± 5 G
$\langle a \rangle_{calc}(^{31}P2)$ = 38 ± 5 G

generated at low temperature (-20 °C). Figure 9 shows its X-band EPR spectrum in THF solution at T = 100 K.

The spectrum in the glassy phase exhibits a metal-in-character line shape which is consistent with a rhombic absorption pattern. The three anisotropic regions exhibit different resolutions of the relevant superhyperfine (shpf) splittings, suggesting a strong interaction of the unpaired electron with the metal coordinating framework in a rather low-symmetry molecular geometry. The actual shpf splittings are suitably interpreted in terms of an $S = ^1/_2$ total electron spin Hamiltonian, taking into account a noticeable magnetic coupling of the electron with two nonequivalent ^{31}P nuclei. As a consequence of this interaction three doublets of doublets are detected, partially overlapped in three 1:2:1 pseudotriplets. Interestingly, there is no EPR evidence for the electron hyperfine coupling of the unpaired electron with the metal-metal center (^{105}Pd, natural abundance = 22%; $I = ^5/_2$). This spectral feature underlines the significant orbital character of the $S = ^1/_2$ monocation line shape. The relevant EPR parameters are summarized in Table III.

Given that the monocation [1]$^+$ substantially maintains the structural geometry of the precursor 1, the appearance of the rhombic line shape suggests an unsymmetrical metal coordination arrangement around the unpaired electron. The second derivative analysis of the spectrum shows the presence of two poorly resolved doublets, centered at g = 2.148 ± 0.005, T = 110 K and at g = 1.898 ± (0.005), T = 160 K, respectively. The interpretation of such absorptions can be made by assuming a significant, but minor, magnetic interaction of the unpaired electron with the ^1H nucleus. The relevant anisotropic shpf coupling constants are

$$a_l(^1H) = 15 ± 5 \text{ G} \qquad a_h(^1H) = 10 ± 5 \text{ G}$$

The lack of the $a_m(^1H)$ signal can be related to solvent effects, mostly affecting the narrowest anisotropic region;
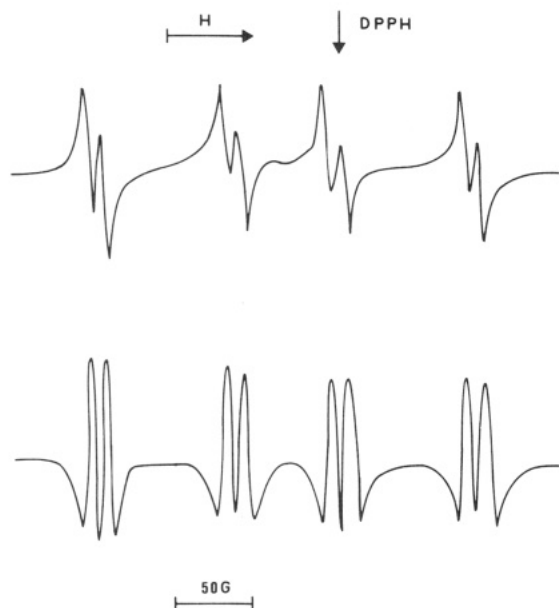
Figure 10. X-Band EPR spectrum of [1]⁺ in THF solution. $T = 250$ K. The upper trace shows the first derivative spectrum, while the second derivative spectrum is shown in the lower trace.

on this basis, by analogy with the previously determined $a_i(^{31}P, ^1H)$ values and by taking into account the relevant ΔH_m value, an upper limit for the actual $a_m(^1H)$ coupling constant can be proposed:

$$a_m(^1H) \leq 12 \pm 5 \text{ G} \leq \Delta H_m$$

Correspondingly, the relevant upper limit for the $\langle a \rangle_{calc}(^1H)$ value is

$$\langle a \rangle_{calc}(^1H) = {}^1/_3(a_l + a_m + a_h) \leq 12 \pm 5 \text{ G}$$

All these data support the assumption of a relatively "long-range" magnetic interaction of the unpaired electron with the ^1H nucleus of the secondary phosphine PBu^t_2H moiety at liquid nitrogen temperature. When the temperature is raised to the glassy/liquid phase transition ($T = 165$ K), the frozen solution spectrum collapses and a new isotropic line shape is evident with a spectral pattern consisting of four unresolved signals. A further increase in temperature induces noticeable line-narrowing (see Figure 10), such that, at $T = 250$ K, the four signals appear well resolved as 1:1 doublets. It is possible that the temperature dependence of the line shape is related to restricted rotation around the $Pd–PHBu^t_2$ bond and/or decreased anisotropy on changing from the glass to liquid state.

The actual spectral features can be interpreted by assuming the interaction of the unpaired electron with two magnetically different ^{31}P nuclei and with one ^1H nucleus; the relevant parameters are

$$\langle g \rangle = 2.026 \pm 0.005 \quad \langle a \rangle(^{31}P1) = 145 \pm 5 \text{ G}$$
$$\langle a \rangle(^{31}P2) = 86 \pm 5 \text{ G}$$
$$\langle a \rangle(^1H) = 12 \pm 5 \text{ G}$$

It is not immediately clear why only two of the four ^{31}P spins interact with the electron. One possible explanation involves fragmentation to a monomeric species containing one terminal secondary phosphine and one bridging phosphide. We do note, however, that Summerville and

Hoffmann,[37] in their theoretical analysis of various transition metal dimers, suggest the following shape for the HOMO's of the phosphido-bridged d^9 dimeric complex $[Rh(CO)_2(PH_2)]_2$
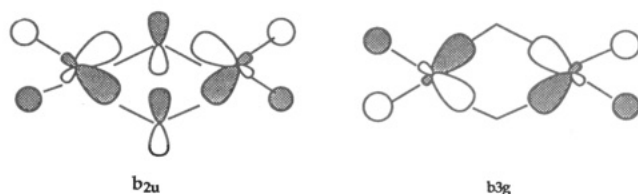
We do not suggest that the above orbitals are appropriate for [1]⁺ (we would expect electron interactions with two equivalent ^{31}P spins in these cases), only that there may be pertinent orbitals with little or no s character with respect to, e.g., a bridging PR_2, with the result that some interactions are very weak. Consequently, we believe that [1]⁺ retains its structural integrity. It is worth repeating that [1]⁺ *is* stable for hours without any sign of decomposition and that the oxidation, in solution, is reversible. One might expect a mononuclear species (which would be strongly coordinatively unsaturated) to be more reactive. In any case, we have no definite proof of structure. We note that the $\langle g \rangle$ data fit well with the corresponding $\langle g \rangle_{calc}$ and the $\langle a \rangle(^1H)$ data also agree with the corresponding $\langle a \rangle_{calc}(^1H)$; in contrast, the $\langle a \rangle_{calc}(^{31}P)$ and the corresponding $\langle a \rangle(^{31}P)$ values noticeably disagree, presumably due to the increase in internal motion and subsequent loss of the anisotropic features when the temperature is raised.

The overall line shape of the X-band EPR spectrum of the frozen THF solution of the deuterium-enriched [1]⁺ species (60%) is not very different from that shown in Figure 9. The relatively broad lines observed might arise due to the three deuterium atoms', I = 1, anisotropic triplet (1:1:1). The actual line shape does not reveal direct EPR evidence for the H to D substitution. Presumably, this is due to the fact that the H-splitting is small to begin with, so that when this is reduced by a factor 6.5 (^2H vs ^1H splitting), the result is a broad line. Consequently, the following statement can be assumed as far as an upper limit for $\langle a \rangle(^2H)$ is concerned:

$$\Delta H_{dd} \geq 2\langle a \rangle(^2H) \quad \langle a \rangle(^2H) \leq 6 \pm 5 \text{ G}$$

Experimental Section

General Data. All manipulations were carried out under a nitrogen atmosphere using standard Schlenk techniques. Complex 1 was prepared as previously described;[12] solvents were dried by conventional procedures and distilled prior to use. IR spectra (Nujol mulls, KBr or CaF_2 plates) were recorded on a Perkin-Elmer FT-IR 1725X spectrometer. NMR spectra were measured using Bruker AC-250 and AMX-500 spectrometers, as described previously.[38,39] Solid-state ^{31}P NMR spectra were recorded on Bruker AC250 and AMX400 spectrometers at 101.2 and 162.0 MHz, respectively, by employing spinning in the magic angle (with frequencies between 5 and 15 kHz) and cross polarization using contact times between 80 μs and 8 ms. ^{31}P NMR data (solid state): (1) 285 (μ-PBu^t_2), 57 ppm ($PHBu^t_2$); ([2]⁺) 445 (μ-PBu^t_2), 230 (μ-$PHBu^t_2$), 52, 48 ppm ($PHBu^t_2$). The instrumentation for the electrochemical and EPR measurements has

(37) Summerville, R. H.; Hoffmann, R. *J. Am. Chem. Soc.* **1976**, *98*, 7240.

(38) Ammann, C. J.; Pregosin, P. S.; Ruegger, H.; Albinati, A.; Lianza, F.; Kunz, R. W. *J. Organomet. Chem.* **1992**, *423*, 415.

(39) Ruegger, H.; Kunz, R. W.; Ammann, C. J.; Pregosin, P. S. *Magn. Reson. Chem.* **1992**, *29*, 197.

Table IV. Experimental Data for the X-ray Diffraction Study of [2a]⁺ and [3a]⁺

compd	[2a]⁺	[3a]⁺
formula	$C_{33}H_{75}F_3O_3P_4Pd_2S$	$C_{27}H_{56}F_3O_5P_3Pd_2S$
mol wt	945.76	855.53
cryst dimens, mm	0.20 × 0.20 × 0.10	0.45 × 0.30 × 0.30
data collecn T, °C	23	23
cryst syst	triclinic	orthorhombic
space group	$P\bar{1}$	$Pbca$
a, Å	10.245(1)	21.910(7)
b, Å	10.739(1)	21.120(3)
c, Å	22.624(3)	16.625(8)
α, deg	79.816(9)	
β, deg	87.876(10)	
γ, deg	68.266(8)	
V, Å³	2274.7(5)	7707(4)
Z	2	8
ρ(calcd), g cm⁻³	1.380	1.477
μ, cm⁻¹	10.02	11.412
radiation (λ, Å)	graphite-monochromated Mo Kα (0.710 69)	
measd reflns	$\pm h, \pm k, +l$	$+h, +k, +l$
θ range, deg	$2.3 < \theta < 23.0$	$2.6 < \theta < 25.0$
scan type	$\omega/2\theta$	$\omega/2\theta$
scan width, deg	$1.10 + 0.35 \tan \theta$	$1.20 + 0.35 \tan \theta$
max counting time, s	75	75
bkgd time, s	0.5 × scan time	0.5 × scan time
max scan speed, deg min⁻¹	6.8	6.8
prescan rejection limit	0.5 (2.00σ)	0.5 (2.00σ)
prescan acceptance limit	0.025 (40.00σ)	0.025 (40.00σ)
horiz receiving slit, mm	$1.70 + \tan \theta$	$1.70 + \tan \theta$
vert receiving slit, mm	4.0	4.0
no. of data collected	6284	6732
no. of obs reflns (n_o) $[|F_o|^2 > 4.0\sigma(|F|^2)]$	4395	3700
transmission coeff	0.9994–0.9601	0.9964–0.9354
decau core	1.0740–0.9948	1.0929–0.9844
no. of params refined (n_v)	375	370
fudge factor f	0.05	0.06
R^a	0.054	0.061
$R_w{}^b$	0.080	0.089
GOF^c	2.295	2.624

^{a} $R = \sum ||F_o| - (1/k)|F_c||/\sum |F_o|$. ^{b} $R_w = [\sum w(|F_o| - (1/k)|F_c|)^2/\sum w|F_o|^2]^{1/2}$, where $w = [\sigma^2(F_o)]^{-1}$ and $\sigma(F_o) = [\sigma^2(F_o{}^2) + f^2(F_o{}^2)^2]^{1/2}/2F_o$. ^{c} GOF $= [\sum w(|F_o| - (1/k)|F_c|)^2/(n_o - n_v)]^{1/2}$.

been described elsewhere,[40] and all of the measured potential values refer to the saturated calomel electrode (SCE).

Preparation of [Pd₂(μ-PBuᵗ₂)(μ-η^2-PBuᵗ₂H)(PHBuᵗ₂)₂]CF₃SO₃, [2a]⁺. CF₃SO₃H (0.070 mL, 0.7 mmol) was added to a suspension of 1 (485 mg, 0.610 mmol) in DME (25 mL). The suspension was refluxed for 24 h giving a deep violet solution. The solution was concentrated to ca. 5 mL, and Et₂O (20 mL) was added. The reaction mixture, which now contained a violet crystalline solid, was cooled to –30 °C for 3 h and the solid was filtered and vacuum dried (yield: 460 mg, 0.486 mmol, 79.7%). Anal. Calcd for $C_{33}H_{75}F_3O_3P_4Pd_2S$: C, 41.9; H, 7.99; P, 13.1; Pd, 22.5. Found: C, 41.5; H, 7.90; P, 12.9; Pd, 22.4. IR (Nujol, cm⁻¹): ν(PH) 2310 (vw, br), 1269 (vs), 1145 (s), 1031 (s), 637 (s). NMR data are given in the text.

Preparation of [Pd₂(μ-PBuᵗ₂)(μ-η^2-PBuᵗ₂H)(PHBuᵗ₂)₂]BF₄, [2b]⁺. HBF₄ (0.160 mL, 54% in Et₂O, d = 1.19 g/mL) was added to a suspension of 1 (426 mg, 0.535 mmol) in DME (25 mL). The resulting suspension was refluxed for 2 h, giving a reaction mixture containing a violet microcrystalline solid. This was cooled to –30 °C for 3 h, and 2b was filtered and vacuum dried (yield: 360 mg, 0.408 mmol, 76.2%). Anal. Calcd for $C_{32}H_{75}BF_4P_4Pd_2$: C, 43.5; H, 8.56; P, 14.0; Pd, 24.1. Found: C, 43.2; H, 8.49; P, 13.7; Pd, 23.9. IR (Nujol, cm⁻¹): ν(PH) 2322 (w), 2301 (w); ν(BF) 1059 (vs).

Preparation of [Pd₂(μ-PBuᵗ₂)(CO)₂(PHBuᵗ₂)₂]CF₃SO₃, [3a]⁺. Saturation of a DME solution of 2a with CO at room

(40) Osella, D.; Ravera, M.; Nervi, C.; Housecroft, C. E.; Raithby, P. R.; Zanello, P.; Laschi, F. *Organometallics* 1991, *10*, 3253.

Table V. Final Positional Parameters and Equivalent Isotropic Displacement Parameters for [2a]⁺ (Esd's Given in Parentheses)

atom	x	y	z	$B,^{a,b}$ Å²
Pd1	0.10390(7)	–0.09011(7)	0.03424(3)	2.34(2)
Pd2	0.93419(7)	–0.51878(7)	0.45613(3)	2.21(2)
S	0.3889(8)	0.9178(8)	0.2798(4)	12.8(2)*
P1	0.2785(3)	–0.2286(3)	0.1062(1)	3.37(7)
P2	0.0468(3)	–0.1063(3)	–0.0650(1)	3.01(6)
P3	0.8071(3)	–0.5132(3)	0.3716(1)	3.80(7)
P4	0.9302(3)	–0.3056(3)	0.4649(1)	2.94(6)
F1	0.453(3)	1.044(2)	0.206(1)	22.9(9)*
F2	0.552(2)	1.055(2)	0.283(1)	20.4(7)*
O1	0.379(3)	0.897(2)	0.352(1)	19.0(8)*
O2	0.246(2)	0.970(2)	0.262(1)	18.5(8)*
O3	0.522(3)	0.842(3)	0.266(1)	25(1)*
C(F1)	0.431(4)	1.062(4)	0.277(2)	21(1)*
C11	0.462(1)	–0.254(1)	0.0834(7)	4.7(3)
C12	0.498(2)	–0.313(2)	0.0263(8)	7.6(5)
C13	0.460(1)	–0.107(1)	0.0689(8)	6.6(4)
C14	0.574(1)	–0.338(2)	0.1310(7)	5.7(4)
C15	0.264(1)	–0.392(1)	0.1438(6)	4.6(3)
C16	0.103(2)	–0.364(2)	0.1513(9)	7.5(5)
C17	0.306(2)	–0.500(2)	0.099(1)	8.6(6)
C18	0.340(2)	–0.447(2)	0.2033(9)	8.3(5)
C21	0.165(1)	–0.086(1)	–0.1282(5)	4.1(3)
C22	0.229(1)	0.017(1)	–0.1103(6)	5.3(3)
C23	0.286(2)	–0.222(2)	–0.1364(7)	6.5(4)
C24	0.079(2)	–0.013(2)	–0.1892(7)	6.4(4)
C25	–0.031(1)	–0.236(1)	–0.0731(5)	3.5(3)
C26	–0.126(1)	–0.236(1)	–0.0187(7)	5.7(3)
C27	–0.124(2)	–0.197(1)	–0.1298(7)	7.2(4)
C28	0.084(2)	–0.380(1)	–0.0709(8)	6.5(4)
C31	0.910(1)	–0.593(1)	0.3120(6)	4.8(3)
C32	1.054(1)	–0.576(2)	0.3118(8)	7.2(4)
C33	0.946(2)	–0.749(2)	0.3234(9)	8.7(5)
C34	0.836(2)	–0.523(2)	0.2469(7)	8.4(5)
C35	0.654(1)	–0.566(1)	0.3863(6)	4.8(3)
C36	0.558(1)	–0.449(2)	0.4262(8)	7.4(5)
C37	0.569(2)	–0.559(2)	0.3331(8)	7.9(4)
C38	0.692(2)	–0.704(2)	0.426(1)	10.4(6)
C41	1.019(1)	–0.222(1)	0.4042(5)	3.7(3)
C42	1.167(1)	–0.341(1)	0.3997(7)	5.3(4)
C43	0.941(2)	–0.185(2)	0.3465(7)	7.1(4)
C44	1.047(2)	–0.104(1)	0.4243(8)	6.7(4)
C45	0.759(1)	–0.182(1)	0.4845(5)	3.6(3)
C46	0.779(2)	–0.074(1)	0.5169(8)	6.9(4)
C47	0.660(2)	–0.109(2)	0.4318(7)	6.5(4)
C48	0.695(1)	–0.267(1)	0.5321(7)	5.5(4)

^{a} Starred values denote atoms refined isotropically. ^{b} Anisotropically refined atoms are given in the form of the isotropic equivalent displacement parameter defined as $^4/_3[a^2\beta_{11} + b^2\beta_{22} + c^2\beta_{33} + ab(\cos \gamma)\beta_{12} + ac(\cos \beta)\beta_{13} + bc(\cos \alpha)\beta_{23}]$.

temperature changed its color from deep to pale violet in a few minutes. This color change was accompanied by a decrease of the intensity of the UV absorption at 535 nm; the equilibrium solution contained ca. 10% of the starting material. Purging the solution with N₂ restores [2a]⁺ quantitatively, and repeated cycles of carbonylation and decarbonylation could be performed without noticeable decomposition. Attempted isolation of solid [3]⁺ under CO atmosphere gave mixtures of [2a]⁺ and [3]⁺ with pure [3]⁺ obtained only occasionally when a minor amount of the compound was precipitated. When the carbonylation was carried out in the presence of excess CF₃SO₃H, the solution turned to bright yellow with complete disappearance of the 535-nm absorption in the UV spectra and up to 20% yields of pure, crystalline [3]⁺ could be precipitated by cooling. If larger amounts of [3]⁺ were precipitated, the coprecipitation of [ᵗBu₂PH₂][CF₃SO₃] was observed. Anal. Calcd for $C_{27}H_{56}F_3O_5P_3Pd_2S$: C, 37.9; H, 6.60; P, 10.9; Pd, 24.9. Found: C, 38.8; H, 6.49; P, 10.7; Pd, 25.0. IR (Nujol, cm⁻¹): ν(CO) 2080 (vs), 2055 (m), 2045 (m), 1270 (vs), 1145 (s), 1130 (s), 635 (s).

[3]⁺ (structure A): ¹H NMR (solution) 4.92 (d × d, 324.0 and 5.3 Hz, PH), 1.43 (AA′XX′, 14.9 Hz, PCH₃ₜ), 1.39 (d, 15.2 Hz, PCH₃ᵦ); ¹³C NMR (solution) 191.6 (d × m, 69 Hz, CO), 41.7

(s, C$_B$), 34.3 (AXX', Σ16.2 Hz, C$_T$), 31.9 (m, CH$_{3B}$), 30.8 (AXX', Σ6.2 Hz, CH$_{3T}$).

[3]$^+$ (structure B): ^{1}H NMR (solution) 4.98 (d × d, 322.0 and 7.6 Hz, PH), 4.87 (d × d, 322.5 and 5.6 Hz, PH), 1.43 (d, 15.2 Hz, PCH$_{3B}$), 1.40 (d, 15.2 Hz, PCH$_{3T}$), 1.37 (d, 14.8 Hz, PCH$_{3T}$); ^{13}C NMR (solution) 193.2 (m, br, CO), 181.9 (d × d × d, 52.5, 16.7, and 9.0 Hz, CO), 43.4 (d, 2.5 Hz, C$_B$), 34.1 (d, 14.3 Hz, C$_T$), 33.4 (d × d, 14.8 and 1.9 Hz, C$_T$), 31.9 (m, CH$_{3B}$), 30.7 (d, 5.7 Hz, CH$_{3T}$), 30.3 (d, 6.2 Hz, CH$_{3T}$).

Preparation of [Pd$_2$(μ-PBu$^t_2$)(CO)$_2$(PHBu$^t_2$)$_2$]BF$_4$, [3b]$^+$. A suspension of [2b]$^+$ in DME (30 mL) was prepared as described above, starting from 487 mg (0.612 mmol) of 1. The suspension, which contained an excess of HBF$_4$·Et$_2$O, was saturated with CO and stirred at room temperature. After 10 min the violet solid had completely dissolved and a white solid precipitated from the yellow-orange solution. The solid was filtered, vacuum dried, and identified as [Bu$^t_2$PH$_2$BF$_4$] from its IR and NMR spectra. The filtrate was concentrated to ca. 10 mL, and Et$_2$O (30 mL) was added; a yellow crystalline solid precipitated, and the suspension was kept at –30 °C overnight. [3b]$^+$ was then filtered and vacuum dried (yield: 393 mg, 0.495 mmol, 81%). Anal. Calcd for C$_{26}$H$_{56}$BF$_4$O$_2$P$_3$Pd$_2$: C, 39.4; H, 7.12; P, 11.7; Pd, 26.8. Found: C, 39.0; H, 7.29; P, 12.1; Pd, 26.5. IR (Nujol, cm^{-1}): ν(CO) 2060 (s), 2025 (m); ν(BF) 1055 (vs).

Reactions of [2a]$^+$ with Bases. DME or THF solutions of [2a]$^+$ were treated with either equimolar amounts of Ph$_3$CLi, a slight excess of LiBEt$_3$H, or a large excess of imidazole. In each case we observed the quantitative precipitation of a red solid, identified as 1 from its IR spectrum.

Decarbonylation of [3b]$^+$. Partial decarbonylation was attempted on DME solutions of [3b]$^+$ by means of the action of vacuum, N$_2$ bubbling, warming, or irradiating with a Helios Italquartz Model UV 13F medium-pressure mercury-vapor arc lamp, and the progress of the reaction was followed by solution IR spectroscopy.

The appearance of new bands of medium intensity in the 2100–2000-cm^{-1} region and of two medium to strong absorptions at 1905 and 1880 cm^{-1} was observed. Prolonged decarbonylation led to complete disappearance of ν(CO) absorptions. Attempted isolation of pure compounds after different degrees of decarbonylation failed and only intractable oils were recovered.

Crystallography

Crystals suitable for X-ray diffraction of [2a]$^+$, deep red in color, were obtained by crystallization from ether, as were those of the yellow compound [3a]$^+$. Complexes [2a]$^+$ and [3a]$^+$ are moderately stable in the air. Crystals of both compounds were mounted on glass fibers, at a random orientation, on an Enraf-Nonius CAD4 diffractometer for the unit cell and space group determinations and for the data collection. Unit cell dimensions were obtained by least squares fit of the 2θ values of 25 high-order reflections (9.5 < θ < 17.3° and 9.5 < θ < 18.4°, respectively) using the CAD4 centering routines. Selected crystallographic and other relevant data are listed in Table IV.

Data were measured with variable scan speed to ensure constant statistical precision on the collected intensities. Three standard reflections were used to check the stability of the crystal and of the experimental conditions and measured every hour. The orientation of the crystal was checked by measuring three reflections every 300 measurements. Data have been corrected for Lorentz and polarization factors and for decay, using the data reduction programs of the MOLEN package.[41] Empirical absorption corrections were applied by using azimuthal (Ψ) scans of four "high-χ" angle reflections (χ > 86°, 8.6 < θ < 17.3° for [2a]$^+$ and χ > 88°, 9.8 < θ < 17.0° for [3a]$^+$). Intensities were considered as observed if $|F_o^2| > 4.0\sigma|F^2|$ and used for the solution and refinement of the structures.

(41) MOLEN. *Molecular Structure Solution Procedure*; Enraf-Nonius: Delft, The Netherlands, 1990.

Table VI. Final Positional Parameters and Equivalent Isotropic Displacement Parameters for [3a]$^+$ (Esd's Given in Parentheses)

atom	x	y	z	B,^{a} Å^2
Pd1	0.16628(5)	0.15034(5)	0.19908(6)	3.06(2)
Pd2	0.08362(5)	0.23677(5)	0.15321(6)	3.11(2)
P1	0.2240(2)	0.0569(2)	0.2129(2)	3.38(8)
P2	0.0869(2)	0.1339(2)	0.1135(2)	2.91(7)
P3	–0.0006(2)	0.2873(2)	0.0939(3)	4.05(9)
O1	0.2325(7)	0.2394(7)	0.3158(9)	9.0(4)
O2	0.1372(7)	0.3454(5)	0.2544(8)	7.0(3)
C1	0.2080(7)	0.2059(8)	0.273(1)	4.8(4)
C2	0.1172(8)	0.3049(8)	0.217(1)	4.8(4)
C11	0.3014(6)	0.0635(9)	0.170(1)	5.0(4)
C12	0.3316(9)	0.1248(9)	0.204(1)	6.8(5)
C13	0.3427(9)	0.009(1)	0.187(1)	7.9(6)
C14	0.289(1)	0.064(1)	0.083(2)	9.0(7)
C15	0.2223(7)	0.0234(7)	0.3175(9)	4.0(3)
C16	0.1590(9)	0.028(1)	0.346(1)	7.5(5)
C17	0.270(1)	0.064(1)	0.370(2)	10.1(8)
C18	0.242(1)	–0.0455(9)	0.320(1)	7.5(6)
C21	0.1021(7)	0.1219(8)	0.0046(9)	4.6(4)
C22	0.0519(9)	0.135(1)	–0.048(1)	6.3(5)
C23	0.1592(9)	0.1690(9)	–0.013(1)	6.0(5)
C24	0.1285(9)	0.0532(8)	–0.014(1)	6.8(5)
C25	0.0260(7)	0.0801(7)	0.1502(9)	3.8(3)
C26	–0.0335(8)	0.092(1)	0.108(1)	6.5(5)
C27	0.0152(6)	0.0966(8)	0.2395(9)	4.4(4)
C28	0.044(1)	0.0121(9)	0.146(1)	6.4(5)
C31	0.0216(9)	0.3540(9)	0.021(1)	6.8(5)
C32	–0.032(2)	0.381(1)	–0.026(2)	8.7(9)
C33	0.059(2)	0.404(1)	0.056(2)	13.3(9)
C34	0.064(2)	0.327(1)	–0.036(2)	12(1)
C35	–0.0615(9)	0.3101(9)	0.172(1)	7.3(5)
C36	–0.034(2)	0.372(1)	0.219(2)	15(1)
C37	–0.068(1)	0.258(1)	0.223(2)	13.8(7)
C38	–0.121(1)	0.331(1)	0.132(1)	11.4(9)
S1	–0.2136(5)	0.3510(6)	0.3887(7)	14.8(4)
O3	–0.198(3)	0.354(3)	0.311(3)	40(3)
O4	–0.1517(8)	0.3545(9)	0.431(1)	11.1(6)
O5	–0.265(1)	0.384(2)	0.428(2)	22(1)
C(F1)	–0.237(2)	0.272(2)	0.379(4)	23(2)
F1	–0.295(2)	0.264(3)	0.368(5)	52(3)
F2	–0.207(2)	0.241(2)	0.365(3)	42(2)
F3	–0.231(2)	0.272(2)	0.482(2)	34(2)

^{a} See footnote b in Table V.

The structures were solved by a combination of Patterson and Fourier methods and refined by full matrix least squares[41] (the function minimized being $\Sigma[w(F_o - 1/kF_c)^2]$). No extinction correction was applied. The scattering factors used, corrected for the real and imaginary parts of the anomalous dispersion,[42] were taken from ref 42.

For the refinement of the structure of [2a]$^+$, anisotropic temperature factors were used for all atoms except those of the anion. The contribution of the hydrogen atoms in calculated positions (C–H = 0.95 Å, B(H) = 1.5B(C$_{bonded}$) Å^2) was taken into account but not refined.

It proved impossible to locate the hydride in the final difference map; therefore possible positions were investigated by a potential energy minima search using the program HYDEX.[43] The lowest minima found (two per each molecule) corresponded to the terminal phosphine hydrogen position and to a location trans to that at approximately 1.9 Å from the Pd and 2.7 Å from the bridging P atom in agreement with the postulated structure.

Final atomic coordinates and equivalent isotropic displacement parameters for 2a are given in Table V.

The refinement of [3a]$^+$ was carried out as above using anisotropic temperature factors for all but the hydrogen atoms. The hydrogen atom contribution (C–H = 0.95 Å, B(H) = 9.0 Å^2) was taken into account but not refined. As can be judged from the value of the thermal parameters, both one phosphine and the

(42) *International Tables for X-ray Crystallography*; Kynoch: Birmingham, England; 1974; Vol. IV.

(43) Orpen, A. G. *J. Chem. Soc., Dalton Trans.* 1980, 2509.

CF$_3$SO$_3$ moiety are disordered. It was not possible to model the different orientations of the sulfonate and only the strongest peaks were retained. Upon convergence the strongest residual peaks (1.25 and 1.10 e A^{-3}, respectively), were around the S and O3 atoms.

Final atomic coordinates and equivalent isotropic displacement parameters for [3a]$^+$ are given in Table VI.

Supplementary Material Available: Tables containing, for structure [3a]$^+$, anisotropic displacement parameters (Table S1), calculated positional parameters for the hydrogen atoms (Table S2), an extended list of bond lengths and angles (Tables S3 and S4), and a list of torsion angles (Table S5) (10 pages). Ordering information is given on any current masthead page. Tables of anisotropic displacement parameters, hydrogen positions, and bond lengths and angles for compound [2a]$^+$ together with the full numbering of the two independent molecules are obtainable as described in ref 14.

OM920555I